Non-Linear Frequency-Domain WEC Simulation: Numerical Case Studies and Practical Issues

Alexis Mérigaud
Centre for Ocean Energy Research (COER),
Maynooth University
Dpt. of Electronic Engineering
Maynooth, Co. Kildare, Ireland
E-mail: alexis.merigaud.2015@mumail.ie

John V. Ringwood
Centre for Ocean Energy Research (COER),
Maynooth University
Dpt. of Electronic Engineering
Maynooth, Co. Kildare, Ireland
E-mail: john.ringwood@nuim.ie

***Abstract*—A non-linear frequency-domain (NLFD) methodology has been recently proposed for the computationally-efficient numerical simulation of wave energy converters (WECs), taking into account non-linear effects in the device dynamics. The primary objective of this paper is to contribute making the wave energy academic and industrial community familiar with the NLFD formulation, by giving researchers and engineers more insight with respect to the practical issues related to the method, as well as its possible application areas. The NLFD method is briefly described, and the main associated practical issues are detailed: robustness and convergence, duration and time-step of the simulations, and finally random generation method for the input wave signal. In terms of WEC dynamics, numerical applications show that NLFD allows for handling strong non-linear dynamics, provided that the WEC outputs remain smooth. The method also allows for modelling cross-frequency energy transfers. In contrast, NLFD does not seem suitable for the non-smooth dynamics related to some specific PTO designs. The small computational time associated with NLFD method makes it particularly advantageous for applications involving a large number of simulations, such as WEC parametric optimisation, power assessment, and WEC dimensioning and reliability.**

***Index Terms*—Wave energy converter, Non-linear model, Numerical simulation, Frequency-domain, Newton method**

I. Introduction

Computationally-efficient WEC modelling is essential in applications requiring a large number of simulations, such as power production assessment, parametric optimisation, or statistical studies. For such applications, high fidelity techniques such as computational fluid dynamics (CFD) are inadequate due to their prohibitive computational costs. Instead, simplified physical models, generally based on linear wave theory, are implemented (see, for example, Chapters 2-4 of [1]).

Amongst the latter, linear WEC models allow for a fast computation of the WEC response in the frequency domain (FD) [2], but their range of applicability is limited to cases where a linear description of the WEC dynamics is accurate. In many practical cases, non-linear modelling of hydrodynamical forces, PTO forces or mooring line effects must be included. In particular, the presence of power-maximising control tends to magnify the non-linearities [3].

Time-domain (TD) numerical integration schemes are generally recommended in the cases where non-linear effects must be taken into account [1]. However, TD integration is significantly slower than linear FD computation, in particular due to the computation of radiation memory terms [4].

Statistical linearisation through the spectral-domain (SD) method [1], [5] allows for the inclusion of velocity-dependent non-linear terms, such as viscous drag, to compute the spectral density function (SDF) of the WEC outputs (displacement or velocity) considered as a Gaussian process. SD linearisation is significantly faster than time-domain integration, but the linearisation methodology cannot be applied to static non-linear terms [6]. Although the resulting linear approximation is optimal in a statistical sense, the linear approximation for non-linear forces makes the method inaccurate for the study of WEC trajectories in the time-domain.

In previous work from the authors [6], a non-linear frequency-domain (NLFD) simulation method has been introduced for wave energy applications. In the NLFD formulation [7], the dynamical equations are projected onto a basis of trigonometric polynomials. The resulting non-linear vector equation is solved through a gradient-based method. In the cases considered in [6], namely, a flap-type WEC with a viscous drag term and a heaving sphere with viscous drag, non-linear restoring force and non-linear control, the proposed technique allows for computing the non-linear WEC steady-state response, both in the frequency domain and in the time domain, at modest computational cost with respect to numerical integration, without compromising the results accuracy.

The objective of this conference paper is to help making the wave energy community familiar with the NLFD formulation, showing its potential applications, as well as the practical issues and limitations associated with the use of the method. More precisely:

- The issues associated with the practical implementation of the NLFD technique are detailed, and largely illustrated throughout the rest of the paper.
- The range of validity, where the NLFD formulation remains efficient, is explored. To this aim, two WEC models are considered: a reactively-controlled spherical heaving point-absorber (HPA) with quadratic viscous drag and a non-linear computation of Froude-Krylov forces, and a cylindrical HPA subject to a Coulomb friction damp-

ing force (resulting from a simplified hydraulic PTO model). The former case, although exhibiting strong non-linearities, can be handled in a computationally-efficient way using NLFD. The latter WEC model, due to the Coulomb-type damping term, has non-smooth outputs, which don't lend themselves easily to a harmonic description. Therefore, the second WEC model represents an example of limit case where using NLFD is not relevant.
- Finally, a range of possible applications of the NLFD framework, along with associated practical issues, is introduced. Three examples are briefly described: WEC parametric optimisation; WEC power assessment; and finally WEC output statistical studies, for example, in the scope of WEC constraint design or fatigue analysis.

The paper layout is as follows: The NLFD method is introduced in Section II, along with the main associated practical issues. The two WEC models considered (spherical and cylindrical heaving point-absorbers) are described in Section III. It is examined, in Section IV, to what extent the NLFD method is suitable for the simulation of both devices. The HPA with Coulomb damping is shown not to lend itself easily to NLFD simulation. Three application examples for the NLFD method (parametric optimisation, power assessment, statistical studies) are detailed in Section V, for the spherical HPA. Finally, the main results of the paper are summarised and discussed in Section VI.

II. Presentation of the NLFD simulation method

For the sake of simplicity, the NLFD method is presented for WECs with one degree of freedom (DoF) only in the present subsection. However, generalisation to more DoFs (or to WECs or WEC farms composed of several interacting bodies) does not pose any theoretical issue [8].

A. NLFD formulation of the WEC dynamics

Let us consider a 1-DoF WEC. The WEC generalised position at a given instant is described by means of a single coordinate ζ. The WEC dynamics are described by the following equation:

$$g_l(\zeta, \dot{\zeta}, \ddot{\zeta}, t) - f_{nl}(\zeta, \dot{\zeta}) = 0 \tag{1}$$

In Eq. (1), g_l includes inertial terms, and forces which depend on ζ and its derivatives in a linear way. For example, if all the hydrodynamic forces acting on the device are linearly modelled, g_l consists of the Cummins equation terms [9]:

$$g_l(\zeta, \dot{\zeta}, \ddot{\zeta}, t) = (\mu+\mu_\infty)\ddot{\zeta} + \int_{-\infty}^{t} k_{rad}(t-\tau)\dot{\zeta}(\tau)d\tau + k_h\zeta - f_e(t) \tag{2}$$

where

- μ is the WEC inertia;
- k_h is a hydrostatic stiffness coefficient;
- the radiation forces are computed as the sum of an inertial term $\mu_\infty\ddot{\zeta}$ and a convolution product between the past values of the velocity and the radiation impulse response function k_{rad};
- f_e is the linear wave excitation force.

The term f_{nl} contains the forces which non-linearly depend on ζ and its derivative. Such a formulation applies to a wide class of semi-analytical WEC models, and allows for the inclusion of various non-linear forces such as non-linear Froude-Krylov forces, quadratic viscous drag, non-linear mooring line effects, non-linear PTO force, etc. Obviously, if a part of the hydrodynamic forces is non-linearly modelled in f_{nl} (e.g. the Froude-Krylov forces), the corresponding terms in (2) have to be removed from the expression of g_l.

A periodic, polychromatic wave signal is now considered. The free-surface elevation is described as a truncated sum of harmonic sinusoids:

$$\eta(t) = \sum_{n=1}^{N} a_{\eta,n}\cos(\omega_n t) + b_{\eta,n}\sin(\omega_n t) \tag{3}$$

where $\omega_n = n\Delta\omega$, and $\Delta\omega$ is the frequency step. The coefficients $a_{\eta,n}$ and $b_{\eta,n}$ can be randomly generated from a wave spectrum, or, alternatively, if the device response to specific frequencies has to be analysed, the coefficients can be non-zeros for just one or several values of n. The projection of η onto the Fourier basis is then

$$E = \begin{bmatrix} a_{\eta,1} & \dots & a_{\eta,N} & b_{\eta,1} & \dots & b_{\eta,N} & 0 \end{bmatrix}^T \in \mathbb{R}^{2N+1} \tag{4}$$

The device dynamical equation (1) is assumed to admit a periodic, continuously-differentiable, steady-state solution, for the periodic input wave signal given in (3). The period of the input and output is then $T = 1/\Delta\omega$ and, for any arbitrary degree of accuracy, all the system variables can be described as truncated sums of sinusoids, similar to (3). As a consequence, (1) can be projected onto the Fourier basis, resulting in:

$$MZ - F_e(E) - F_{nl}(Z, E) = 0_{\mathbb{R}^{2N+1}} \tag{5}$$

where

- Z denotes the projection of the coordinate ζ onto the trigonometric basis:

$$Z = \begin{bmatrix} a_{\zeta,1} & \dots & a_{\zeta,N} & b_{\zeta,1} & \dots & b_{\zeta,N} & a_{\zeta,0} \end{bmatrix}^T \tag{6}$$

- MZ is the projection of the linear terms of g_l which depend on ζ and its derivatives. In particular, using Ogilvie's relation [10], the linear time-domain radiation terms simplify into the frequency-dependent radiation added mass and damping $A_{rad}(\omega)$ and $B_{rad}(\omega)$. Typically, when both radiation and hydrostatic restoring forces are linearly modelled, the components of M are given, $\forall i, j \in [\![1...N]\!]^2$, as

$$\begin{aligned} M_{i,j} &= \begin{cases} -\omega_i^2(\mu + A_{rad}(\omega_i)) + k_h, & i = j \\ 0, & i \neq j \end{cases} \\ M_{i+N,j+N} &= M_{i,j} \\ M_{i,j+N} &= \begin{cases} \omega_i B_{rad}(\omega_i), & i = j \\ 0, & i \neq j \end{cases} \\ M_{i+N,j} &= -M_{i,j+N} \\ \text{and } M_{2N+1,2N+1} &= k_h \end{aligned} \tag{7}$$

- The term $F_e(E)$ denotes an additive force term. If the excitation forces are linearly modelled, then F_e corresponds to the excitation term of g_l, and can be derived from E using the linear excitation force transfer function. If the totality, or a part of the excitation forces are non-linearly modelled, F_e is an additive term which depends on E in a linear or non-linear way.
- $F_{nl}(Z,E)$ is the projection of the non-linear forces f_{nl} onto the trigonometric basis, so that $\forall i \in [\![1...N]\!]$:

$$F_{nl,i}(Z,E) = \frac{2}{T}\int_0^T f_{nl}(\zeta_Z, \dot{\zeta}_Z, \eta_E)\cos(\omega_i t)dt$$
$$F_{nl,i+N}(Z,E) = \frac{2}{T}\int_0^T f_{nl}(\zeta_Z, \dot{\zeta}_Z, \eta_E)\sin(\omega_i t)dt \quad (8)$$
$$F_{nl,2N+1}(Z,E) = \frac{1}{T}\int_0^T f_{nl}(\zeta_Z, \dot{\zeta}_Z, \eta_E)dt$$

  where the subscript notation indicates that the periodic, time-domain signals ζ_Z and its derivative depend on the components of Z, in a way analogous to (3).

B. Solution method

The dynamical equations are now expressed as (5), which, for a given input E, is a non-linear vector equation of the form

$$G(Z) = 0 \quad (9)$$

A Newton method can be used to solve (9). In particular, for a given vector Z, the Jacobian matrix $J_G(Z)$ of G can be explicitly derived, as detailed in [7]. Then, an approximate solution of (9) is found by iteratively solving

$$G(Z^{(n)}) + J_G(Z^{(n)})(Z^{(n+1)} - Z^{(n)}) = 0_{\mathbb{R}^{2N+1}} \quad (10)$$

until $\|G(Z)\|^2$ becomes smaller than a given threshold.

C. Practical issues

The main practical issues associated with the use of the NLFD method are described in this subsection. Most of them will be exemplified in Sections IV and V.

1) Initialisation and convergence issues: The initialisation is instrumental in achieving a fast convergence of the method. Typically, solving for the linearised dynamical equation (setting F_{nl} to zero or approximating it in a linear way) can provide a judicious starting point for the algorithm. In some cases, however, other initial guesses can be considered. For example, concerning a heaving point-absorber, the wave elevation itself can be used as a starting point.

Solving (9) using a simple Newton method is subject to two main drawbacks:

- Convergence cannot be guaranteed, especially if the starting point of the algorithm is too far from the actual solution [11]. Even for relatively simple non-linear functions, such as polynomials in just one or two dimensions, the domain of convergence of Newton method is a complicated mathematical problem.
- The Jacobian $J_G(Z)$ may be badly conditioned, in which case the inversion problem (10) cannot be solved.

In order to enforce convergence, and ensure that the iterative problem (10) is well-conditioned, more sophisticated root-finding algorithms can be considered. For example, the algorithms available in the commercial software MATLAB[1], are the trust-region, the trust-region dogleg, and the Levenberg-Marquardt methods. For such techniques, the explicit Jacobian computation as in [7] remains valuable since, otherwise, the Jacobian is evaluated less accurately through finite differences.

2) Number, length and time-step of the simulations: The Jacobian computation, at each iteration of the algorithm, requires $2N+1$ fast Fourier transforms (FFTs). As a consequence, the computational time:

- depends on the size of the problem, in $N^2\ln(N)$;
- increases linearly with the number of iterations before convergence is achieved.

Therefore, the size of the problem has to be as small as possible, without compromising the result accuracy. Specifically, N is determined as $N = T \times f_{max}$, where :

- The simulation length, T, which is also the period of the generated signal, determines the frequency step $\Delta f = 1/T$. Too short a signal means that the frequency contents of inputs and outputs are poorly represented. In contrast, a long signal deteriorates the NLFD computational performance. Therefore, for the same total simulated time, many, relatively short simulations, should always be privileged over fewer, longer runs, under the condition that the frequency discretisation is accurate enough.
- The cut-off frequency f_{max} is related to the time step as $f_{max} = 1/(2\Delta t)$. Even if the input wave spectrum is zero for frequencies above f_{max}, non-linearities may result in the WEC outputs having significant non-zero components beyond f_{max}. Therefore, if f_{max} is chosen too small (or equivalently Δt too big), high-frequency dynamics cannot be properly represented, and the algorithm may fail in finding a solution with an error $\|G(Z)\|^2$ lower than the target threshold. In contrast, choosing an excessively small time step represents an unnecessary computational burden, when the corresponding high frequencies are not present in the device dynamics.

3) Random input generation: Another important factor to consider is the way the amplitudes of the input wave components are randomly generated. In most works in the wave energy sector, the coefficients $a_{\eta,n}$ and $b_{\eta,n}$ of (3) are randomly generated, following a "deterministic amplitude scheme" (DAS), as $a_{\eta,n} = \cos(\Phi_n)\sqrt{2S(f_n)\Delta f}$ and $b_{\eta,n} = -\sin(\Phi_n)\sqrt{2S(f_n)\Delta f}$, where $S(f)$ is the spectral density function of the wave elevation process, and each Φ_n is randomly chosen following a uniform distribution in $[0; 2\pi]$.

[1] https://uk.mathworks.com/help/optim/ug/equation-solving-algorithms.html

However, as explained in [12] and [13], in order to truly represent the randomness of a Gaussian sea sampled over a finite time duration, $a_{\eta,n}$ and $b_{\eta,n}$ should be chosen, following a "random amplitude scheme" (RAS), as $a_{\eta,n} = \alpha_n\sqrt{S(f_n)\Delta f}$ and $b_{\eta,n} = \beta_n\sqrt{S(f_n)\Delta f}$, where each α_n and β_n is randomly chosen following a standard normal distribution.

Although RAS is statistically correct, and thus may be required for the study of specific statistical properties of the WEC inputs or outputs, DAS has the advantage that power estimates (calculated over the whole period of the generated signal) present a significantly smaller variance than with RAS[2]. However, it has to be ensured that the power estimates using DAS do not introduce any significant bias, with respect to RAS results.

Finally, regardless of the use of either DAS or RAS, the statistical effect of the signal periodicity upon the outputs of interest has to be carefully taken into account. If necessary, the first or last part of each simulation may be discarded, in order to avoid the unrealistic correlation between the first and last points of the simulation [13].

III. Numerical WEC models

A. Heaving point-absorber with non-linear Froude-Krylov forces

The WEC considered in this subsection is a spherical heaving point-absorber, subject to reactive control, and for which Froude-Krylov pressure forces are integrated over the instantaneous wetted surface. This case study illustrates the capability of the NLFD formalism to handle strong static and velocity-dependent non-linear effects.

The only degree of freedom is in heave, and ζ denotes the vertical coordinate of the device gravity centre ($\zeta = 0$ in hydrostatic equilibrium).

The radiation and diffraction forces are modelled in a linear way, using hydrodynamic coefficients obtained from the hydrodynamic software NEMOH[3].

Assuming infinite water depth, static and dynamic Froude-Krylov forces are integrated analytically over the instantaneous wetted surface of the sphere, similarly to [14]. However, a more efficient implementation of the method into the NLFD formalism involves a finite-order development of the dynamic Froude-Krylov forces, described in more detail in the appendix of [15]. Furthermore, a Wheeler stretching is applied to the expression of the pressure field as a function of depth, so that the total of the static and incident pressures is actually zero at the free surface.

Finally, for a given irregular wave train characterised by complex amplitudes $A(\omega)$ and wave numbers $k(\omega)$, the static Froude-Krylov force can be expressed as:

$$\vec{F}_s(\zeta',t) = \rho g\pi\big[\frac{2}{3}R^3 - R^2\zeta' + \frac{1}{3}\zeta'^3 - \eta(t)(R^2-\zeta'^2)\big]\vec{u}_z \quad (11)$$

and the dynamic Froude-Krylov forces can be developed as

$$\vec{F}_{dyn}(\zeta',t) = \big[I_{-1}(t)\zeta' + I_{-2}(t) - \sum_{n=0}^{\infty} J_n(t)\zeta'^n\big]\vec{u}_z \quad (12)$$

where ζ' denotes the position of the gravity centre relatively to the free surface, and $\forall n \in \mathbb{Z}$,

$$I_n(t) = 2\pi\rho g \int_0^{\infty} \Re\{A(\omega)\mathrm{e}^{\jmath\omega t}\}k(\omega)^n d\omega \quad (13)$$

and, $\forall n \in \mathbb{N}$,

$$\begin{aligned} J_n(t) =& \frac{2\pi\rho g}{n!}\int_0^{\infty} \Re\{A(\omega)\mathrm{e}^{\jmath\omega t}\} \\ &\times \big(\frac{R}{k(\omega)} + \frac{1}{k(\omega)^2}\big)\mathrm{e}^{-k(\omega)R}k(\omega)^n d\omega, \end{aligned} \quad (14)$$

For a given, finite set of random complex wave amplitudes, the terms $I_{-1}(t)$, $I_{-2}(t)$ and $J_n(t)$ are computed prior to simulation, by means of FFTs. In practice, the magnitude of J_n decreases quickly with the order n, which makes it sufficient to develop (12) up to $n = 2$ or $n = 3$ only.

Viscous effects are modelled through a quadratic term of the form $f_v(\dot{\zeta}) = -B_v|\dot{\zeta}|\dot{\zeta}$.

The PTO force is composed of two terms: a linear damping term $-B_{PTO}\dot{\zeta}$, and a non-linear static restoring term of the form $u_s(\zeta)$. The latter is a reactive control term, adapted to the case where the WEC cross-sectional area is not constant:

$$u_s(\zeta) = \begin{cases} \frac{K_{PTO}}{R^2}(\frac{1}{3}\zeta^3 - R^2\zeta) & \zeta \in [-R;R] \\ -\frac{2}{3}K_{PTO}R & \zeta \geq R \\ \frac{2}{3}K_{PTO}R & \zeta \leq -R \end{cases} \quad (15)$$

As explained in [6] and [15], similarly to linear reactive control, u_s enables to tune the device dynamics to the incident wave period, on a sea-state by sea-state basis, while allowing the control force and device motions to remain within reasonable limits, in most cases. Fig. 1 shows the non-linear static control force, as well as a non-linear static restoring force for a spherical point-absorber.

A linear version of the spherical HPA is also implemented (with linear hydrostatic restoring force and excitation force, and with linear reactive control). More detail about the sphere hydrodynamic model can be found in the Appendix of [15].

The presence of a reactive control term requires that some care be taken, when physically interpreting the simulation results. In the linear case, for example, if the PTO reactive term is set at a higher value than the hydrostatic stiffness, the total stiffness of the system is negative, which can lead to unrealistic motions. With non-linear Froude-Krylov forces and restoring terms, similar limitations must be expected, as will be illustrated in V-A, although the physical interpretation is significantly more complicated.

[2]The variance of the estimate obtained using DAS is even zero when the WEC model is linear [13]

[3]https://lheea.ec-nantes.fr/doku.php/emo/nemoh/start

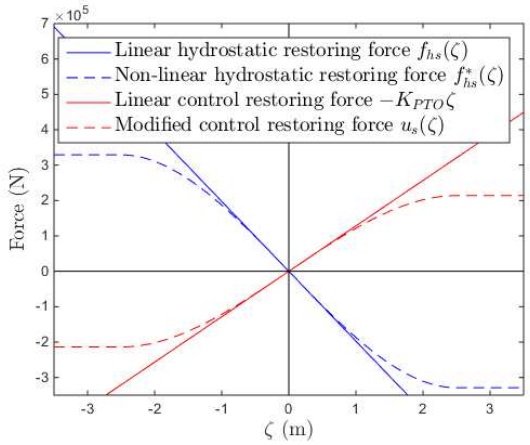

Fig. 1. Linear and non-linear hydrostatic restoring force and PTO restoring force models

B. Heaving point-absorber with Coulomb damping

The second WEC studied is a heaving cylinder, connected to a hydraulic PTO system. The hydrodynamic model of the cylinder is represented linearly, with frequency-domain coefficients computed using the hydrodynamic software NEMOH[4].

The behaviour of the hydraulic PTO system is derived by [16], in the simple case where the PTO resisting force Φ is assumed to be constant. In this condition, the PTO force acting on the device acts as a Coulomb damper: when the WEC is moving, the PTO exerts a resisting force $f_{PTO} = -\Phi \text{sign}(\dot{\zeta})$ ("slip condition"). However, whenever the WEC velocity goes to zero, the device stops moving ("stick condition") until the sum of all hydrodynamic forces overcomes Φ.

WEC motions corresponding to such a physical model are non-smooth, and thus do not lend themselves easily to a representation through a finite harmonic series. In a time-domain simulation, the stick condition can be forced by means of a simple *if* condition. In the NLFD formulation, the PTO force is more problematic. In particular, the derivative $\partial f_{PTO}/\partial\dot{\zeta}$, required to compute the Jacobian J_G, is not defined in $\dot{\zeta} = 0$. Therefore, the function $f_{PTO}(\dot{\zeta}) = -\Phi \text{sign}(\dot{\zeta})$ can be approximated by means of a function

$$f^*_{PTO}(\dot{\zeta}) = -\Phi \tanh(\alpha\dot{\zeta}), \tag{16}$$

where the parameter α determines the accuracy of the approximation.

IV. Numerical simulation results: NLFD capabilities and limitations

A. Spherical heaving point-absorber

The spherical heaving point-absorber is simulated in two conditions:

- a monochromatic, sinusoidal input wave with a 8 s period and a 2 m amplitude;
- a JONSWAP [17] spectrum with $H_s = 2$ m and $T_p = 8$ s.

[4]https://lheea.ec-nantes.fr/doku.php/emo/nemoh/start

In both cases, the PTO parameters B_{PTO} and K_{PTO} are manually set up so as to ensure resonance of the device in the incoming wave - and hence magnify the non-linear effects.

Two simple initial guesses are considered for the solution of the dynamical equations: the output for the linear WEC model, and the free surface itself. Interestingly, the former generally yields faster convergence (in only 2 iterations) but, in a small minority of cases, causes the simple Newton algorithm to fail in converging. This is because the solution of the linear model leads to large-amplitude WEC motions (the device being at times entirely emerged): with such extreme initial solutions, it might happen, either that the Jacobian $J_G(Z)$ be ill-conditioned, or that the initial solution be outside the domain of convergence of the Newton algorithm. In contrast, choosing the free surface as initial solution allows for systematic convergence of the method (generally in 3 iterations), and is then selected.

In order to choose the parameters T and f_{max} (see II-C), the polychromatic case is considered. It is found that increasing T beyond 120 s does not bring any significant change in power estimates, and that $\Delta t = 1/2f_{max} = 0.6$ s suffices to capture the device dynamics. Therefore the cut-off frequency is $1/2\Delta t \approx 0.83$Hz, and the frequency step is $1/T = 0.0083$Hz, so that the frequency range (from 0 to 0.83 Hz) is discretised into 100 frequencies.

With the settings described above in terms of initial solution and problem size, the NLFD algorithm converges quickly. Running a large number of simulations, it is found that the time per simulation is between 0.017 and 0.018 s (using a 3.50 GHz, 8-core Intel® processor), so that obtaining the equivalent of one hour of WEC output (i.e. 30 short simulations) only takes approximately 0.5 s. For comparison, employing a second-order Runge-Kutta (RK2) method, with a time-step of 0.01 s and using direct computation of radiation forces, is found to be between 50 and 60 times slower.

1) Response to monochromatic waves: The response of a linear WEC model to a monochromatic wave is a sinusoid with the same frequency as the input wave. In contrast, with non-linear WEC models, there can be transfers of energy across frequencies. The NLFD methodology allows for modelling such non-linear cross-frequency transfers, which is illustrated as follows: the spherical heaving point-absorber is simulated, using NLFD, in a monochromatic input wave (with a 2-m amplitude and a period approximately equal to 8 s). The output of NLFD is given as a vector containing all the Fourier components of the periodic, steady-state solution. Therefore, the amplitude of the sinusoidal components at each frequency can be readily computed, and compared with the linear response.

Fig. 2 shows the frequency-domain amplitude components for the input wave elevation and for the WEC motion, obtained from the linear and non-linear WEC models. Of course, the input contains only one non-zero component, and so does the linear WEC motion. The linear WEC motion amplitude is twice the one of the wave, showing the resonance achieved by the reactive control. The non-linear WEC response also shows resonance at the wave frequency, with an amplitude

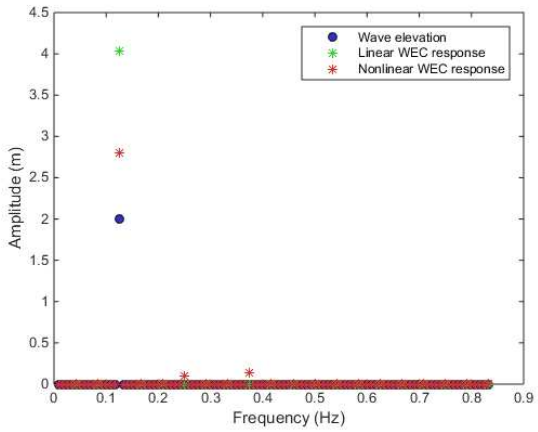

Fig. 2. Linear and non-linear WEC frequency-domain response to a monochromatic input wave

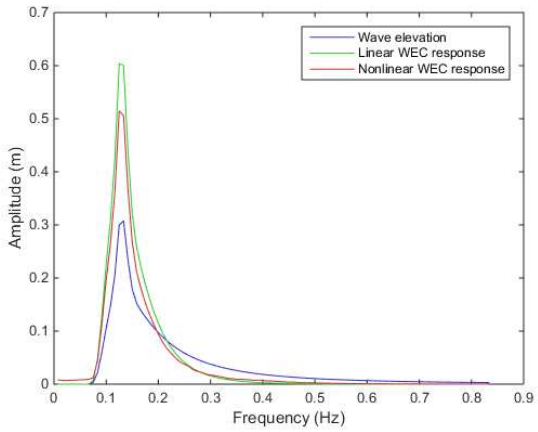

Fig. 3. Linear and non-linear WEC frequency-domain response to a JONSWAP spectrum

significantly larger than the wave - but not as large as the linear response. Furthermore, non-zero components can be observed outside the input wave frequency. Only two are clearly visible on Fig. 2 (located at multiples of the input frequency), but closer examination shows that a significant number of other frequency components are non-zero. Hence, NLFD allows for modelling the cross-frequency transfers due to the presence of non-linear forces.

2) Response to polychromatic waves: Similarly to the monochromatic case, the frequency-domain response of the device to a JONSWAP spectrum can be estimated, using just a couple of NLFD simulations. The amplitude responses for both the linear and non-linear WEC models are shown in Fig. 3, where it can be seen that the presence of non-linearities significantly distorts the output amplitude spectrum.

Finally, applying a simple FFT to the frequency-domain outputs of the NLFD algorithm, the WEC motions can be analysed in the time domain. As an illustration, Fig. 4 compares the time-domain response of the non-linear spherical WEC, obtained through NLFD and through RK2, as well as the response of the linear WEC model.

The strong discrepancy between the linear and non-linear results shows the importance of modelling non-linear effects in this specific case (with reactive control making non-linear effects more significant). The non-linear WEC responses, obtained through numerical integration and NLFD, only differ during the transient time (since, with NLFD, only the steady-state response is computed).

B. Heaving point-absorber with non-smooth motion

The cylindrical HPA is simulated in a JONSWAP spectrum with $H_s = 1$m and $T_p = 8$s. For the NLFD computation, the *sign* function is approximated as in (16), with different α values, while in the time-domain integration, the stick condition is implemented by means of an *if* loop. The simulation time is set to $T = 100$s. Δt is set to a relatively small value of 0.25 s to allow for approximating non-smooth motions.

When the occurrence of stick condition becomes significant, i.e. for relatively high values of α and Φ, the simple Newton algorithm fails in converging. Therefore, the more robust trust-region dogleg method, readily-implemented in the commercial software MATLAB, is used to solve for (9).

Fig. 5 shows the time-domain integration results, as well as the NLFD results for a small and a high value of α. It can be seen that with $\alpha = 10$s/m, the approximation is poor with respect to the correct dynamics (obtained through time-domain integration). With higher values of α (such as $\alpha = 200$s/m in this example), the approximation improves significantly, although still departing from the correct dynamics at times.

In terms of computational time, with $\alpha = 10$s/m, the NLFD method is two times faster than RK2 integration, but with $\alpha = 200$s/m, the NLFD computational time is twice the one of RK2. For NLFD to approximate better the correct, sharp-edged motions, the parameter α should be increased, as well as the cut-off frequency, at additional computational cost. Overall, NLFD is not a suitable simulation method for WECs with such non-smooth outputs.

V. Examples of Applications

In this section, we show how the NLFD method can be used for different types of applications: parametric optimisation, statistical studies, and power assessment. Only the spherical point-absorber is considered.

A. Parametric optimisation

In this subsection, the NLFD method is used in order to optimise the non-linear PTO parameters B_{PTO} and K_{PTO} in a JONSWAP sea state with $H_s = 2$m and $T_p = 8$s. A simple exhaustive search approach is used, within which a discrete range of K_{PTO} and a range of B_{PTO} values are defined, and the WEC power output is evaluated for each K_{PTO}, B_{PTO} pair.

There are 18 values for K_{PTO}, and 13 values for B_{PTO}. Furthermore, for the average power estimate to be reliable, 10

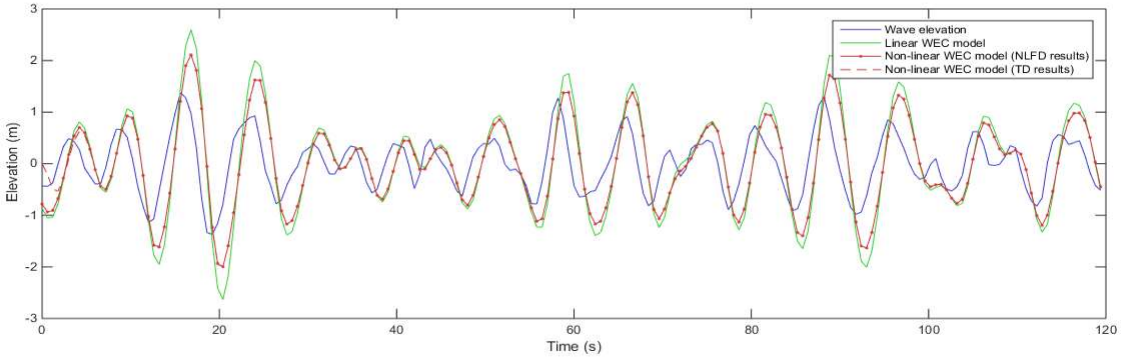

Fig. 4. Time-domain response for the linear WEC model, and time-domain response of the non-linear WEC model computed using NLFD and TD integration

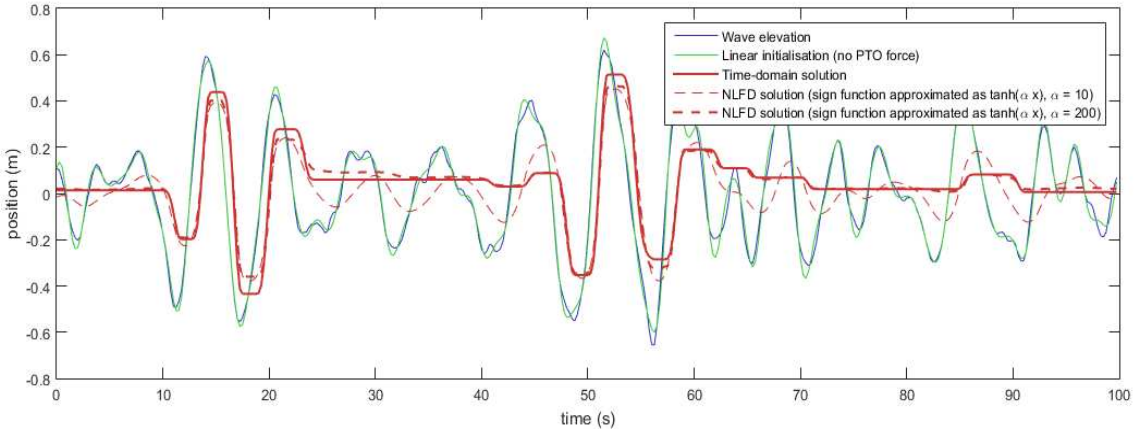

Fig. 5. Time-domain response for the cylindrical point-absorber

simulations of length 120 s are run for each PTO combination. Thus, there are in total 2340 simulations to run (corresponding to more than 3 days of cumulative simulation time).

The result, in terms of average power output for each PTO setting, is shown on Fig. 6. The time per simulation is 0.018 s, for a total time of 40 s. 3 or 4 iterations are generally necessary to achieve convergence. However, for strong reactive term values and small damping values, close to the optimal setting, the simple Newton algorithm can fail in converging.

For those K_{PTO}, B_{PTO} combinations where convergence is not achieved, closer analysis is carried out by considering time-domain results: the NLFD results (not converged) are shown on Fig. 7, along with the trajectory obtained through RK2. The results suggest that some specific PTO settings tend to make the WEC system unstable. Therefore, the convergence issue in the NLFD algorithm can be related to the instability of the physical model, and cannot necessarily be overcome by means of a basic time-domain integration method.

As in Section IV-B, the more robust trust-region dog-leg method, readily-implemented in the commercial software MATLAB, can be used to solve the NLFD problem, when the simple Newton method fails. However, the average computa-

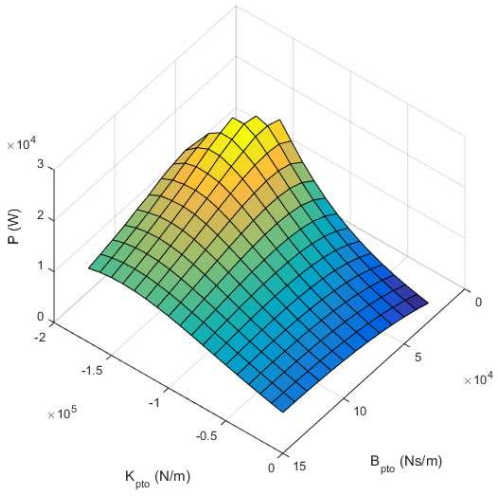

Fig. 6. Average WEC power across the K_{PTO}, B_{PTO} space

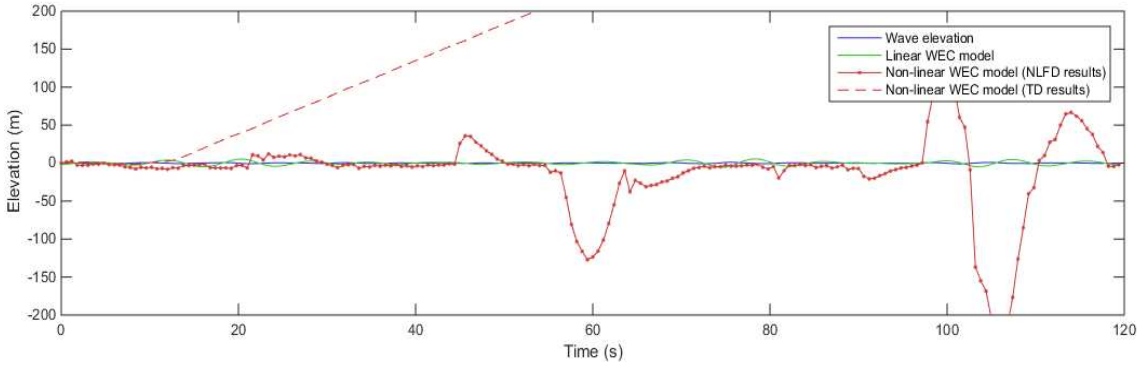

Fig. 7. Time-domain response for the spherical HPA for unstable PTO settings

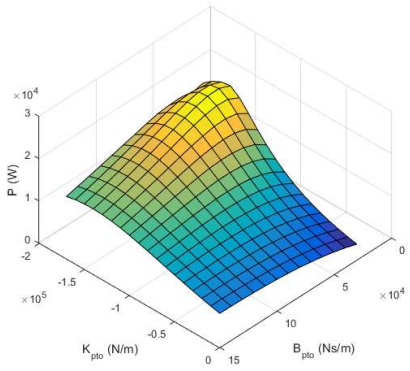

Fig. 8. Average WEC power across the K_{PTO}, B_{PTO} space (robust solution)

tional time per simulation becomes approximately 4 to 5 times larger than for the simple Newton algorithm. Therefore, the two methods are rather used in a complementary fashion, the robust trust-region method being only used as a last resort, when the simple Newton algorithm has not converged. The computational time per simulation can thus be contained to approximately 0.03 s.

Finally, an additional improvement consists of choosing the initial solution of each NLFD simulation in a more clever way. Indeed, the same 10 sets of random phases can be used for all the PTO combinations (i.e. all the K_{PTO}, B_{PTO} combinations are evaluated in the same wave signals). For a given set of random phases, i.e. the same input wave signal, the solutions of the dynamical equation for two neighbouring PTO settings are likely to be close to each other. In order to exploit this idea, the optimisation is now implemented in the following form: For each set of random phases, and for each B_{PTO} value, K_{PTO} is gradually incremented, and (9) is solved, using as initial solution the result for the previous K_{PTO} value (or the free-surface itself for the first K_{PTO} value).

In this way, the average number of iterations is reduced, and the computational time per simulation is brought down from 0.03 to approximately 0.025 s, which makes it possible to carry out the exhaustive search, in a robust way, in less than one minute. The corresponding results, now computed over the whole parametric space, are shown in Fig. 8. In comparison, RK2 is estimated to be approximately 40 times slower (and is not robust to "extreme" PTO settings around the optimum).

B. Power assessment

Another purpose for which numerous simulations are necessary is WEC power assessment. The general methodology consists of using historical wave data for a specific location, over typically a year or more, and estimating the average WEC power output during the chosen duration. At every time step of the period considered, i.e. typically every 1-3 hours, the power output is computed from the knowledge of the wave spectrum. As a consequence, power assessment involves the computation of the WEC output in a large number of sea states, which is carried out, in most studies, using the power matrix device representation.

However, power matrices assume that all sea states can be represented as parametric spectra, such as JONSWAP [17] or Bretschneider [18]. As pointed out in [19], the resulting error in power output calculations can be significant for some WEC types and locations. Computationally efficient power output calculation in each individual spectrum can avoid such errors.

As an illustration, Fig. 9 compares, for 3-hourly sea states, the output predicted by a power matrix, with the output estimated in the actual sea states by means of NLFD simulations. The wave data was recorded in 2010 in Belmullet, and provided by the Irish Marine Institute[5]. The WEC model considered is the same spherical HPA, with reactive control, as in [15]. The use of a power matrix leads to significant error, both on a sea-state by sea-state and on an annual basis. As in [19], the broadness parameter ϵ_0 is indicated on the figure, to show that the error committed using a power matrix tends to be larger for broader spectra, i.e. those which depart the most from standard spectral shapes.

[5]http://www.marine.ie/Home/site-area/data-services/real-time-observations/wave-buoys

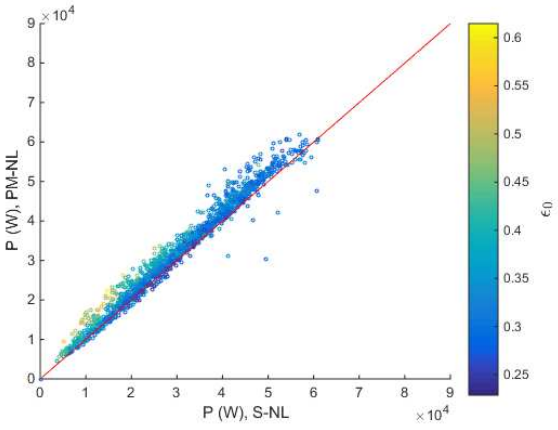

Fig. 9. Power output in each sea state, using a power matrix *vs* simulations in the actual spectra

In terms of computational time, the NLFD technique makes it possible to evaluate the power output, for all the 1500 three-hourly spectra of the data set, in no more than 3 minutes.

C. Statistical studies

WEC design should aim at maximising power production, while ensuring WEC survivability and limiting capital costs. To this end, in addition to average power extraction, a variety of other statistical measures of the WEC dynamics can be useful at the WEC design stage. When defining the WEC operational range and dimensioning its components, accurate knowledge of the statistical distribution of specific variables, such as displacement, velocity, forces, or instantaneous power, in given sea conditions, constitutes important information.

For example, in studies such as [19], [20], the device response amplitude operator (RAO) or its operational range (in terms of sea condition) are limited, based on the probability of exceeding some position threshold. The calibration of such limitations could be usefully informed by a more accurate consideration of the WEC non-linear dynamics, as illustrated in Fig. 10(a), which shows the empirical probability density function of the WEC position in a JONSWAP sea state with $H_s = 2$m and $T_p = 8$s. In a similar fashion, Figs. 10(b) and 10(c) could be used to define the dimensions of the PTO system and of the generator.

WEC reliability assessment, for example in the framework of a failure mode effects analysis (FMEA) [21], could also take profit from extensive WEC simulation in order to estimate the probability of failure of various components. Other statistics, such as cycle counting, are also instrumental in detailed WEC structural design, for fatigue analysis in particular (see Chapter 14 of [1]), and can also be derived empirically from numerous WEC simulations in design sea states.

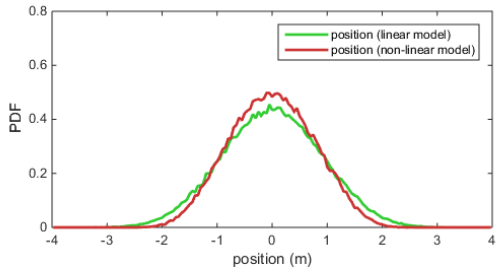

(a) SDF of the WEC position

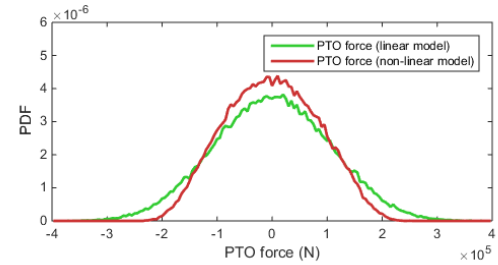

(b) SDF of the PTO force

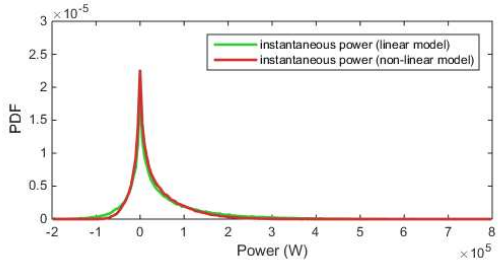

(c) SDF of the instantaneous absorbed power

Fig. 10. Empirical probability density function (PDF) of various physical variables, obtained using $120 \times 500 = 60,000$ s of simulation

VI. Discussion and Conclusions

A. NLFD and practical issues

It has been shown how a NLFD formulation can be used to transform the dynamical equation into a non-linear vector equation, which can be efficiently solved using gradient-based zero-finding algorithms. The main practical issues associated with the use of the NLFD simulation method are the possible convergence problems of the chosen solution algorithm, the settings related to problem sizing (length and sampling time of the input periodic signal), and the method for random wave input generation.

In particular, to take full advantage of the NLFD formulation in terms of computational time, many, relatively short simulations should always be favoured over fewer, longer ones (for the same total simulated time); however, it has to be ensured that the corresponding frequency discretisation does not introduce any significant error in the WEC output.

Where necessary, robustness issues can be overcome through more sophisticated root-finding algorithms than a

simple Newton method, at the expense of less computational efficiency.

B. Range of capabilities

In terms of WEC dynamics, NLFD allows for handling strong non-linear dynamics, provided that the WEC outputs remain smooth, i.e. continuously differentiable. The method also allows for modelling cross-frequency energy transfers.

In contrast, the NLFD does not seem suitable for the non-smooth dynamics related to some specific PTO designs. More generally, a detailed analysis of PTO components is likely to include high-frequency dynamics, for which the NLFD formulation may not be particularly relevant in comparison to time-domain numerical integration.

Finally, considering the Coulomb damping (Section IV-B) and the parametric optimisation (Section V-A) examples, it is interesting to note that it seems to be more difficult for the algorithm to find a solution to the non-linear dynamical equation, when the underlying physical model becomes more "extreme", nay unstable. In particular, the algorithm may not converge if the dynamical equation do not admit a steady-state solution. Thus, the existence and significance of the NLFD results depend on the consistency of the underlying analytical physical model, which must then be carefully designed.

C. Application examples

The small computational time associated with NLFD method makes it particularly suitable for applications involving a large number of simulations.

In parametric optimisation, the modest computational time of NLFD brings the exploration of a wide range of parameters within computational reach, while preserving a suitable representation of non-linear effects. Furthermore, for small, gradual variations in the parameters, and using the same input waves, it is possible to use the NLFD solution as initial condition for a neighbouring set of parameters, which can considerably enhance the computational performance.

For WEC power assessment, using NLFD to carry out extensive WEC simulation, in every individual sea state, can usefully avoid the errors associated with the use of a power matrix, while taking into account non-linear dynamics, at a limited computational expense.

NLFD simulations could also bring more insight into studies related to the WEC dimensioning and reliability: the modifications of the output statistics induced by non-linear effects can be duly represented; furthermore, a large set of time-domain trajectories can be easily obtained in a short amount of time, which can be used for fatigue analysis.

ACKNOWLEDGMENT

This paper is based upon work supported by Science Foundation Ireland under Grant No. 12/RC/2302 for the Marine Renewable Ireland (MaREI) centre.

REFERENCES

[1] M. Folley, *Numerical Modelling of Wave Energy Converters*. Academic Press, 2016.

[2] J. Falnes, *Ocean waves and oscillating systems: linear interactions including wave-energy extraction*. Cambridge University Press, 2002.

[3] M. Penalba Retes, A. Mérigaud, J.-C. Gilloteaux, and J. Ringwood, "Nonlinear froude-krylov force modelling for two heaving wave energy point absorbers," in *Proceedings of the 11th European Wave and Tidal Energy Conference*. European Wave and Tidal Energy Conference 2015, 2015.

[4] J. A. Armesto, R. Guanche, F. Del Jesus, A. Iturrioz, and I. J. Losada, "Comparative analysis of the methods to compute the radiation term in cummins equation," *Journal of Ocean Engineering and Marine Energy*, vol. 1, no. 4, pp. 377–393, 2015.

[5] M. Folley and T. Whittaker, "Spectral modelling of wave energy converters," *Coastal Engineering*, vol. 57, no. 10, pp. 892–897, 2010.

[6] A. Mérigaud and J. V. Ringwood, "A non-linear frequency-domain approach for numerical simulation of wave energy converters," *IEEE Trans. on Sustainable Energy*, Revised manuscript submitted Apr. 2017.

[7] P. Spanos, M. Di Paola, and G. Failla, "A Galerkin approach for power spectrum determination of nonlinear oscillators," *Meccanica*, vol. 37, no. 1-2, pp. 51–65, 2002.

[8] G. Failla, P. Spanos, and M. Di Paola, "Response power spectrum of multi-degree-of-freedom nonlinear systems by a Galerkin technique," *Journal of Applied Mechanics*, vol. 70, no. 5, pp. 708–714, 2003.

[9] W. Cummins, "The impulse response function and ship motion," *Schiffstechnik*, no. 9, pp. 101–109, 1962.

[10] T. Ogilvie, "Recent progress toward the understanding and prediction of ship motions." in *Sixth Symposium on Naval Hydrodynamics*, 1964.

[11] M. S. Bazaraa, H. D. Sherali, and C. M. Shetty, *Nonlinear Programming: Theory and Algorithms*. John Wiley & Sons, 2013.

[12] J.-B. Saulnier, A. Clément, F. d. O. António, T. Pontes, M. Prevosto, and P. Ricci, "Wave groupiness and spectral bandwidth as relevant parameters for the performance assessment of wave energy converters," *Ocean Engineering*, vol. 38, no. 1, pp. 130–147, 2011.

[13] A. Mérigaud and J. V. Ringwood, "Free-surface time-series generation for wave energy applications," *IEEE Journal of Oceanic Engineering*, Accepted Feb. 2017.

[14] G. Giorgi and J. V. Ringwood, "Computationally efficient nonlinear froude–krylov force calculations for heaving axisymmetric wave energy point absorbers," *Journal of Ocean Engineering and Marine Energy*, pp. 1–13, 2016.

[15] A. Mérigaud and J. V. Ringwood, "Power production assessment for wave energy converters: Overcoming the perils of the power matrix," *Part M: Journal of Engineering for the Maritime Environment, SAGE Publishing*, Submitted March 2017.

[16] A. Falcão, "Modelling and control of oscillating-body wave energy converters with hydraulic power take-off and gas accumulator," *Ocean Engineering*, vol. 34, no. 14, pp. 2021–2032, 2007.

[17] K. Hasselmann, T. Barnett, E. Bouws, H. Carlson, D. Cartwright, K. Enke, J. Ewing, H. Gienapp, D. Hasselmann, P. Kruseman *et al.*, "Measurements of wind-wave growth and swell decay during the Joint North Sea Wave Project (JONSWAP)," pp. 1–95, 1973.

[18] C. Bretschneider, "Wave variability and wave spectra for wind generated gravity waves," Beach Erosion Board, US Army Corps of Eng., Washington, DC, Tech. Rep. 118, 1959.

[19] A. De Andrés, R. Guanche, J. Weber, and R. Costello, "Finding gaps on power production assessment on wecs: Wave definition analysis," *Renewable Energy*, vol. 83, pp. 171–187, 2015.

[20] J. Goggins and W. Finnegan, "Shape optimisation of floating wave energy converters for a specified wave energy spectrum," *Renewable Energy*, vol. 71, pp. 208–220, 2014.

[21] M. Mueller, R. Lopez, A. McDonald, and G. Jimmy, "Reliability analysis of wave energy converters," in *Renewable Energy Research and Applications (ICRERA), 2016 IEEE International Conference on*. IEEE, 2016, pp. 667–672.